

Vertebrate POLQ and POL β Cooperate in Base Excision Repair of Oxidative DNA Damage

Michio Yoshimura,^{1,2,10} Masaoki Kohzaki,^{1,3}
Jun Nakamura,⁴ Kenjiro Asagoshi,⁵ Eiichiro Sonoda,¹
Esther Hou,⁵ Rajendra Prasad,⁵ Samuel H. Wilson,⁵
Keizo Tano,³ Akira Yasui,⁶ Li Lan,⁶ Mineaki Seki,⁷
Richard D. Wood,⁷ Hiroshi Arakawa,⁸
Jean-Marie Buerstedde,⁸ Helfrid Hohegger,¹
Takashi Okada,^{1,9} Masahiro Hiraoka,²
and Shunichi Takeda^{1,*}

¹Department of Radiation Genetics, CREST
Japan Science and Technology Laboratory
Graduate School of Medicine
Kyoto University

Yoshida Konoe, Sakyo-ku
Kyoto 606-8501

²Department of Radiation Oncology and
Image-Applied Therapy
Graduate School of Medicine
Kyoto University

54 Shogoin Kawaharacho, Sakyo-ku
Kyoto 606-8507

³Research Reactor Institute
Kyoto University

2 Asashironishi, Kumatoricho
Sennan-gun

Osaka 590-0494
Japan

⁴Department of Environmental Sciences
and Engineering

The University of North Carolina
Chapel Hill, North Carolina 27599

⁵Laboratory of Structural Biology, NIEHS
National Institutes of Health
Research Triangle Park, North Carolina 27709

⁶Department of Molecular Genetics
Institute of Development, Aging, and Cancer
Tohoku University
Seiryomachi 4-1
Sendai 980-8575
Japan

⁷University of Pittsburgh
Hillman Cancer Center
5117 Centre Avenue
Research Pavilion Suite 2.6
Pittsburgh, Pennsylvania 15213

⁸Institute of Molecular Radiobiology, GSF
Ingolstädter Landstrasse 1
D-85764 Neuherberg, Munich
Germany

⁹Department of Urology
Graduate School of Medicine
Kyoto University
54 Shogoin Kawaharacho, Sakyo-ku
Kyoto 606-8507
Japan

Summary

Base excision repair (BER) plays an essential role in protecting cells from mutagenic base damage caused by oxidative stress, hydrolysis, and environmental factors. POLQ is a DNA polymerase, which appears to be involved in translesion DNA synthesis (TLS) past base damage. We disrupted POLQ, and its homologs HEL308 and POLN in chicken DT40 cells, and also created *polq/hel308* and *polq/poln* double mutants. We found that *POLQ*-deficient mutants exhibit hypersensitivity to oxidative base damage induced by H₂O₂, but not to UV or cisplatin. Surprisingly, this phenotype was synergistically increased by concomitant deletion of the major BER polymerase, POL β . Moreover, extracts from a *polq* null mutant cell line show reduced BER activity, and POLQ, like POL β , accumulated rapidly at sites of base damage. Accordingly, POLQ and POL β share an overlapping function in the repair of oxidative base damage. Taken together, these results suggest a role for vertebrate POLQ in BER.

Introduction

Base excision repair (BER) is a crucial process that eliminates many types of base damage that arise endogenously (Lindahl, 1993). Typically, BER begins with a lesion-specific DNA glycosylase that eliminates the damaged base from the deoxyribose of DNA strands (Barnes and Lindahl, 2004). Strand incision is carried out by some glycosylases involved in the repair of oxidative damage as well as AP endonuclease. The resulting single-strand breaks (SSBs) are filled either with one nucleotide (single-nucleotide [SN] BER or short-patch BER) or with several nucleotides leading to displacement of the parental strand (long patch [LP] BER). This DNA synthesis involves POL β (Sobol et al., 2000), but other polymerase or polymerases are likely to play an important role in this pathway as well, because a defect in POL β has little impact on cell proliferation (Sobol et al., 1996), whereas loss of the major AP endonuclease activity is incompatible with viability (Izumi et al., 2005). BER also processes base damage caused by the oxidative agent, hydrogen peroxide (H₂O₂), as well as monofunctional alkylating agents, such as methyl methane-sulfonate (MMS) (Lindahl, 2000).

The *Drosophila melanogaster* (Dm) *MUS308* gene is a DNA polymerase containing a helicase domain at the N terminus. *mus308* mutants are hypersensitive to DNA crosslinking agents such as nitrogen mustard and cisplatin (CDDP) without displaying marked sensitivity to MMS (Boyd et al., 1990). The human genome database analysis reveals a close homolog of *MUS308*, designated *POLQ* (*POL θ*), which encodes 2590 amino acid residues and belongs to the A type family of DNA polymerases (Seki et al., 2003, 2004). In addition, two vertebrate *POLQ* paralogs were identified; *HEL308* shows homology to the helicase domain of *POLQ* (Marini and Wood, 2002) but has no polymerase domain, while *POLN* shows homology to the polymerase domain of

*Correspondence: stakeda@rg.med.kyoto-u.ac.jp

¹⁰Present address: Department of Radiology, Kurashiki Central Hospital, Miwa 1-1-1, Kurashiki 710-8602, Japan.

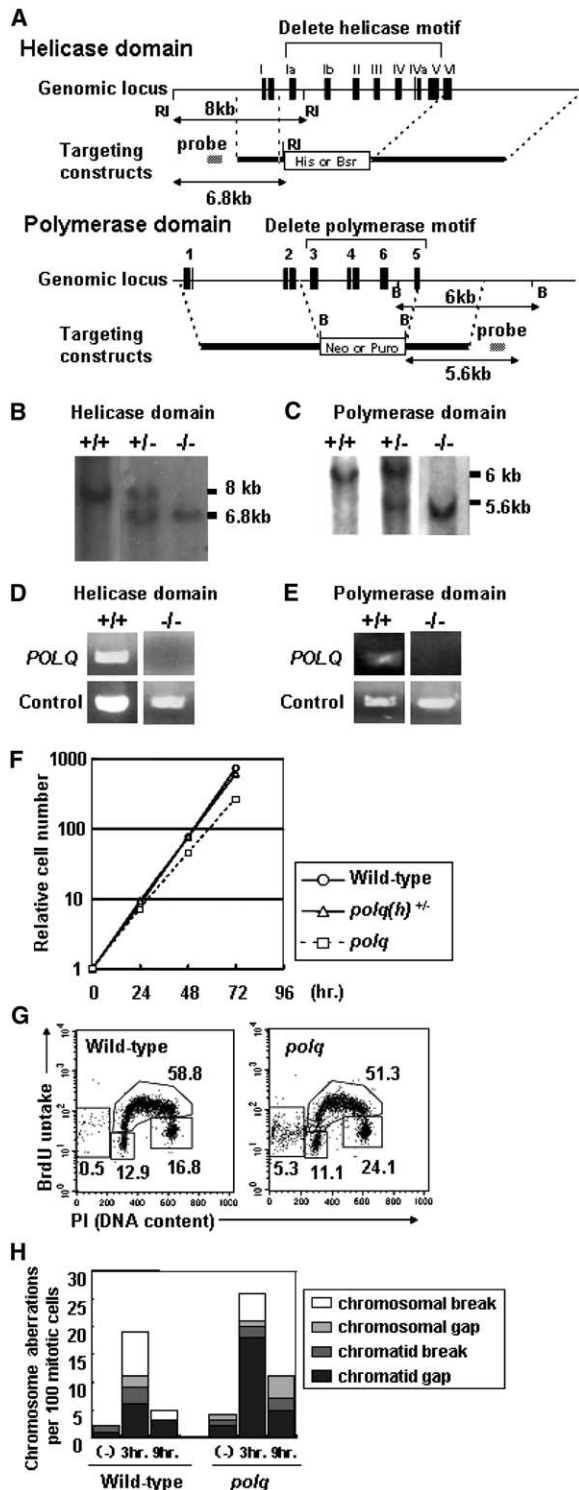


Figure 1. Experimental Strategy and Gene Targeting of *POLQ* Locus (A) Schematic representation of restriction map of the helicase and the polymerase domain of the chicken *POLQ* locus, and the gene disruption construct.

(B and C) Southern blot analysis of EcoRI-digested genomic DNA from cells with the indicated genotypes of the helicase domain, and BamHI-digested genomic DNA from cells with the indicated genotypes of the polymerase domain, using the probe shown in (A). EcoRI digestion causes 8 kb and 6.8 kb fragments and BamHI digestion causes 6 kb and 5.6 kb fragments in wild-type and targeted alleles, respectively.

POLQ but has no helicase domain (Marini et al., 2003). Subsequently, biochemical studies showed that both *POLQ* and *POLN* have DNA polymerase activity and that *HEL308* exhibits helicase activity (Seki et al., 2003, 2004). Furthermore, *POLQ* can perform translesion DNA synthesis (TLS) past AP sites and thymine glycol adducts (Seki et al., 2004). However, the function of these *POLQ* paralogs in vivo has not been identified. The analysis of *polq*-deficient mice revealed a moderate change in the pattern of immunoglobulin (Ig) V hypermutation, suggesting that *POLQ* may play a role in TLS or BER (Masuda et al., 2005; Ukai et al., 2006; Zan et al., 2005).

To investigate the function of these *POLQ*-related genes in vertebrate cells, we generated cells deficient in both the helicase and polymerase domains of the *POLQ* gene (hereafter abbreviated as *polq* cells), as well as single domain disrupted clones from the chicken B lymphocyte line, DT40 (Hochegger et al., 2004; Yamazoe et al., 2004). We furthermore generated cells deficient in the helicase domains of both *POLQ* and *HEL308* genes (hereafter called *polq/hel308* cells), and cells deficient in the polymerase domains of both *POLQ* and *POLN* (hereafter called *polq/poln* cells). We also deleted the *POLβ* gene in *polq* cells to make *polq/polβ* double null cells. In this study, we report an unexpected finding of redundant functions for *POLQ* and *POLβ* in BER.

Results

Generation of *polq*, *polq/hel308*, and *polq/poln* Mutants

Similar to the human and mouse *POLQ* loci (Seki et al., 2004), the chicken *POLQ* locus contains a helicase-like domain and a polymerase domain. Amino acid sequence conservation between chicken and human *POLQ* is 78% identity and 94% similarity within the helicase-like domain, and 72% identity and 92% similarity within the polymerase domain. We generated gene-targeting constructs of the helicase and polymerase domains in the *POLQ* gene to delete seven helicase motifs (Ia, Ib, II, III, IV, IVa, and V) and four DNA polymerase motifs (3, 4, 6, and 5), respectively (Figure 1A). We also made gene-targeting constructs of *HEL308* to delete

(D and E) RT-PCR analysis to verify inactivation of the *POLQ* gene. RT-PCR analysis of purified total RNA from wild-type and homozygous mutant cells. PCR amplification was carried out with primers hybridizing with coding sequences that are deleted by gene targeting.

(F) Growth kinetics of *polq* cells. Each value represents the mean of relative cell numbers from three independent experiments. (G) Cell-cycle analysis. Representative cell-cycle distribution of the indicated cell cultures as measured by BrdU incorporation (vertical axis, log scale) and DNA content (horizontal axis, linear scale) in flow cytometric analysis. Numbers show the percentages of cells falling in each gate.

(H) Level of chromosomal aberrations in mitotic cells. Cytologically detectable chromosome aberrations were measured in 100 mitotic cells for each preparation. The level of spontaneous aberrations is indicated as (-). To measure IR-induced chromosomal breaks, asynchronous populations of cells were exposed to 2 Gy γ rays, followed by harvesting mitotic cells at 3 hr and 9 hr post IR. Cells were exposed to colcemid for the last 3 hr prior to cell harvest to enrich mitotic cells.

Table 1. Frequency of Spontaneous Chromosomal Aberrations in Wild-Type and *polq* Cells

Cell (Clone Name)	Number of Cells Analyzed	Chromatid Type		Chromosome Type		Chromatid Exchanges		Total (Per Cell)
		Gaps	Breaks	Gaps	Breaks	Gaps	Breaks	
Wild-type	100	1	1	0	0	0	0	2 (0.02)
<i>polq</i>	100	2	1	1	0	0	0	4 (0.04)

eight helicase motifs (I, Ia, Ib, II, III, IV, IVa, and V) (see Figure S1A in the Supplemental Data available with this article online), and of *POLN* to target the first polymerase motif (Figure S1B).

To study the function of vertebrate POLQ, we isolated two clones, in which the helicase domain in the *POLQ* locus was replaced by selection marker genes (hereafter called *polq[h]* cells) (Figures 1B and 1D). These disrupted clones showed increased sensitivity only to H₂O₂, but not to other damaging agents, such as chemical crosslinking agents (data not shown). To exclude aberrant expression of the remaining part of the gene, we also disrupted the POLQ polymerase domain in the two *polq(h)* cell lines to generate two *polq* clones (Figures 1C and 1E). Moreover, to investigate a functional overlap between *POLQ* paralogs, we generated *polq/hel308* and *polq/poln* cells (Figure S1). We found that *polq(h)*, *polq*, and the two double mutants all exhibited a very similar phenotype as judged by their growth properties and cellular sensitivity to DNA-damaging agents (Figure S2 and data not shown), and we hereafter describe the phenotype of the two *polq* clones.

The growth properties of *polq* cells were monitored by measuring growth curves and by cell-cycle analysis. *polq* cells grew slower, remained longer in G₂ phase than wild-type cells (Figure 1F), and had an increased sub-G₁ fraction indicating spontaneous cell death (Figure 1G). This phenotype is consistently observed in DT40 mutant clones that display genome instability (Sonoda et al., 2003). Likewise, *polq* cells exhibited a modest increase in the level of spontaneous chromosomal breaks (Table 1 and Figure 1H). Furthermore, *polq* cells showed an elevated level of spontaneous sister chromatid exchange (SCE) (Figure S3A), which reflects genome instability during replication, when compared with wild-type cells. These data indicate that POLQ plays a role in maintaining chromosomal DNA stability during the cell cycle.

POLQ Deficiency Causes an Increase in Sensitivity to Killing by H₂O₂, but Not by Chemical Crosslinking Agent

To assess the DNA-repair capacity of *polq* cells, we examined viability of the cells after various genotoxic treatments using colony-survival assays. *polq* cells showed no significant increase in sensitivities to chemical crosslinking agents, such as CDDP and mitomycin C (MMC), to UV irradiation, or to γ rays, when compared with wild-type cells (Figures 2A–2D). Likewise, neither *polq/hel308* nor *polq/poln* double mutant showed hypersensitivity to these DNA-damaging agents (Figures S2A and S2B). Furthermore, chromosomal aberrations induced by 2 Gy γ rays were comparable between wild-type and *polq* cells (Figure 1H). We therefore conclude that the POLQ family of proteins does not significantly contribute to cellular tolerance to either ionizing radia-

tion or crosslinking agents. This is in marked contrast to the hypersensitivity of the *Drosophila mus308* mutant to interstrand crosslinking agents.

Conversely, *polq* cells were hypersensitive to H₂O₂, which causes oxidation at purines (e.g., 7,8-dihydro-8-oxoguanine (8-oxoG), pyrimidines (thymine glycol), and abasic sites (Lindahl, 2000; Nakamura et al., 2000), but did not show hypersensitivity to MMS (Figures 2E and 2F). The level of H₂O₂-induced SCE was indistinguishable between wild-type and *polq* cells (Figure S3B). The deletion of *HEL308* or *POLN* in *polq* cells did not increase the sensitivity to H₂O₂ or render the cells MMS sensitive (data not shown). In contrast, cells deficient in *POL β* , the major BER polymerase, showed hypersensitivity only to MMS, but not to H₂O₂ (Figures 2E and 2F) (K.T., H.A., E.S., J.A. Swenberg, J.-M.B., S.T., M. Watanabe, and J.N., unpublished data). Thus, both *POL β* and POLQ may contribute to BER, which repairs lesions induced by MMS and H₂O₂. Alternatively, *POL β* and POLQ may participate in different repair pathways, with POLQ being involved in TLS as suggested by biochemical studies (Seki et al., 2004). To test this hypothesis, we generated *polq/pol β* cells to understand the functional interactions of these two polymerases. Remarkably, *polq/pol β* displayed significantly higher sensitivity to MMS than either single mutant (Figure 2E). Thus, a defect in *POL β* unmasks a role for POLQ in cellular tolerance to MMS. We observed a similar effect of the *POL β* gene disruption in the *polq* mutant background, on the sensitivity to oxidative DNA damage, induced by 5-hydroxymethyl-2'-deoxyuridine (HmdUrd) (Figure 2G). HmdUrd is incorporated into genomic DNA by replication, subsequently recognized by uracil-DNA glycosylases, and eventually eliminated by the BER pathway (Braithwaite et al., 2005; Matsubara et al., 2004). Thus, POLQ and *POL β* might function in a common pathway, with POLQ acting as a backup for *POL β* in cellular resistance to MMS- and HmdUrd-induced DNA damage. Alternatively, defective TLS in *polq* and impaired BER in *pol β* might have a synergistic effect on cellular survival following exposure to exogenous DNA damage. In the case of H₂O₂, the double mutant did not show a further increase in sensitivity when compared to *polq* cells (Figure 2F). From these data, it cannot be determined in which repair pathway POLQ participates to deal with oxidative damage induced by H₂O₂.

Decreased In Vitro SN BER of Oxidative Base Damage in the Absence of POLQ

To examine a possible role of POLQ in BER, we performed an in vitro SN BER assay using a 35 bp oligonucleotide that contained either uracil (Figures 3A–3D) or 8-oxoG (Figures 3E–3H) (Biade et al., 1998; Braithwaite et al., 2005), a typical method to induce base damage by oxidation (Lindahl, 1993). In this way, we measured the SN BER capacity of various DT40 cell extracts,

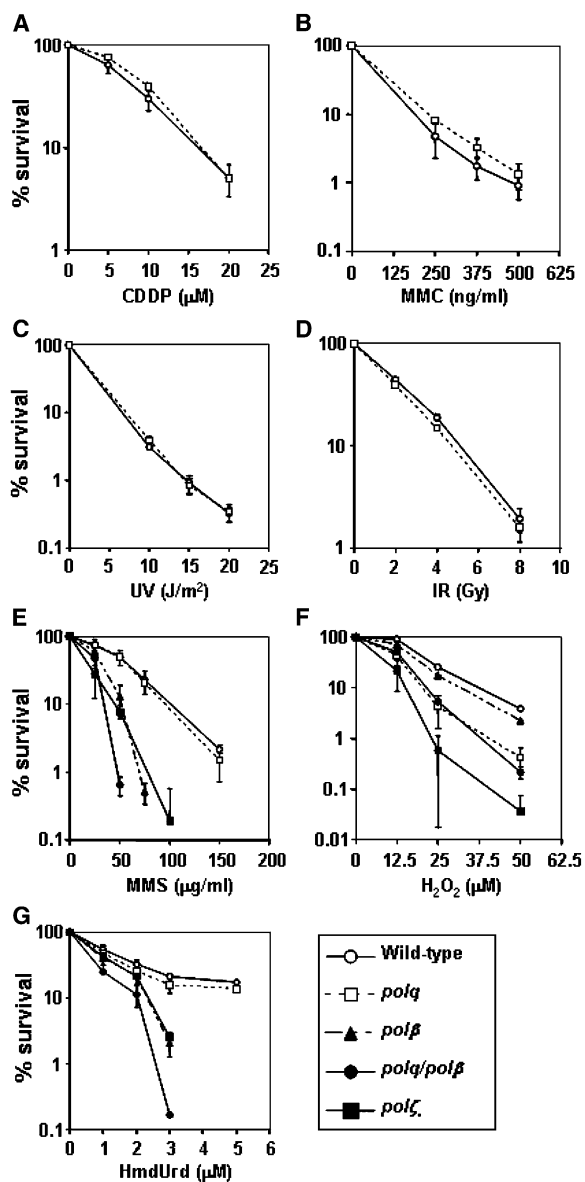


Figure 2. Sensitivities of *polq* Cells to Killing by Various DNA-Damaging Agents

The indicated genotypes of cells were exposed to (A) CDDP, (B) MMC, (C) UV, (D) γ rays (IR), (E) MMS, (F) H_2O_2 , and (G) HmdUrd. The doses and concentrations (conc.) of genotoxic agents are displayed on the x axis in a linear scale, while the fractions of surviving colonies are displayed on the y axis in a logarithmic scale. Error bars show the SD of the mean for at least three independent experiments. Plating efficiencies of wild-type and mutant cells were $\sim 100\%$.

including wild-type, *polβ*, *polq*, and *polq/polβ* cells. The *polβ* mutant extract showed $\sim 50\%$ reduction in BER activity as compared to that of wild-type cell extract (Figure 3D). This result is consistent with previous observations (Sobol et al., 2000) and with the mutant's MMS sensitivity (Figure 2E). Thus, POL β appears to be a major BER polymerase in DT40 as well as mammalian cells. Interestingly, the POLQ-deficient extract showed a reduction in BER capacity similar to that shown by the POL β -deficient extract (Figures 3C and 3D). This result suggests that POLQ also contributes significantly to

SN BER. Furthermore, the BER capacity of the *polq/polβ* double null extract was reduced to a near-background level, indicating an additive effect of gene deletion of these polymerases. Taken together, these results suggest that POLQ may be involved in BER.

In addition to a role of POLQ in uracil-mediated BER, we also investigated the role of POLQ in 8-oxoG-mediated BER. To this end, a 34 bp oligonucleotide containing 8-oxoG was incubated with DT40 cell extracts (Figures 3E–3H). While cell extracts deficient in POL β showed a modest reduction in BER capacity ($\sim 25\%$), cell extract prepared from the *polq* mutant cell line showed more than 50% reduction in BER capacity. This result suggests a role of POLQ in 8-oxoG repair. This result correlates well with the colony survival of *polq* mutants after H_2O_2 treatment, which induces 8-oxoG lesions in DNA by oxidation of guanines (Figure 2F).

POLQ Contributes to Both SN BER and LP BER

Next, we wanted to investigate whether POLQ is involved in LP as well as SN BER. To analyze these two types of BER separately, a uracil-containing oligonucleotide-based assay, shown in Figure 3A, was modified, so that the second nucleotide incorporated by repair DNA synthesis was a chain terminating ddTMP instead of a normal dTMP. Thus, single-nucleotide DNA synthesis followed by ligation with the downstream 20 nt strand may produce 35 bp SN BER product, while longer DNA synthesis may produce 16 bp product, which represents a LP BER intermediate (Figure 4A). We performed these experiments with extracts prepared from wild-type and *polq* mutant DT40 cells, as shown in Figures 4B–4D. The activity of both SN and LP BER was several-fold reduced in the absence of POLQ (Figure 4B). In addition, depletion of POLQ seemed to reduce LP BER more significantly than SN BER (Figures 4C and 4D).

To confirm these results, we employed a plasmid-based assay. A uracil-containing plasmid was incubated with DT40 cell extracts, and DNA synthesis corresponding to either a single nucleotide or two and more nucleotides during BER was separately measured. To this end, we quantified the incorporation of [^{32}P]dCMP in the 25 bp KpnI-XhoI fragment reflecting the sum of SN and LP BER and in the 16 bp XhoI-KpnI fragment reflecting only LP BER (Figure 4E). A representative autoradiograph is displayed in Figure 4F, and the average proportions of SN BER and LP BER in wild-type and *polq* cell extracts are shown (Figure 4G). The proportion of LP BER in the *polq* and wild-type cell extracts was 6% and 12%, respectively.

In summary, biochemical analysis suggests that POLQ contributes to uracil-initiated BER pathway at the same level as does POL β (Figures 3A–3D) and plays a more important role in BER of 8-oxoG than does POL β (Figures 3E–3H). The data from the oligonucleotide substrate (Figures 4A–4D) and the plasmid substrate (Figures 4E–4G) consistently show the involvement of POLQ in LP BER as well as SN BER.

Increase in the Level of Unrepaired SSBs in *polq/polβ* Cells Compared to *polβ* Cells Following Exogenous Base Damage

To further address the putative involvement of POLQ in BER, we attempted to measure the level of SSBs and

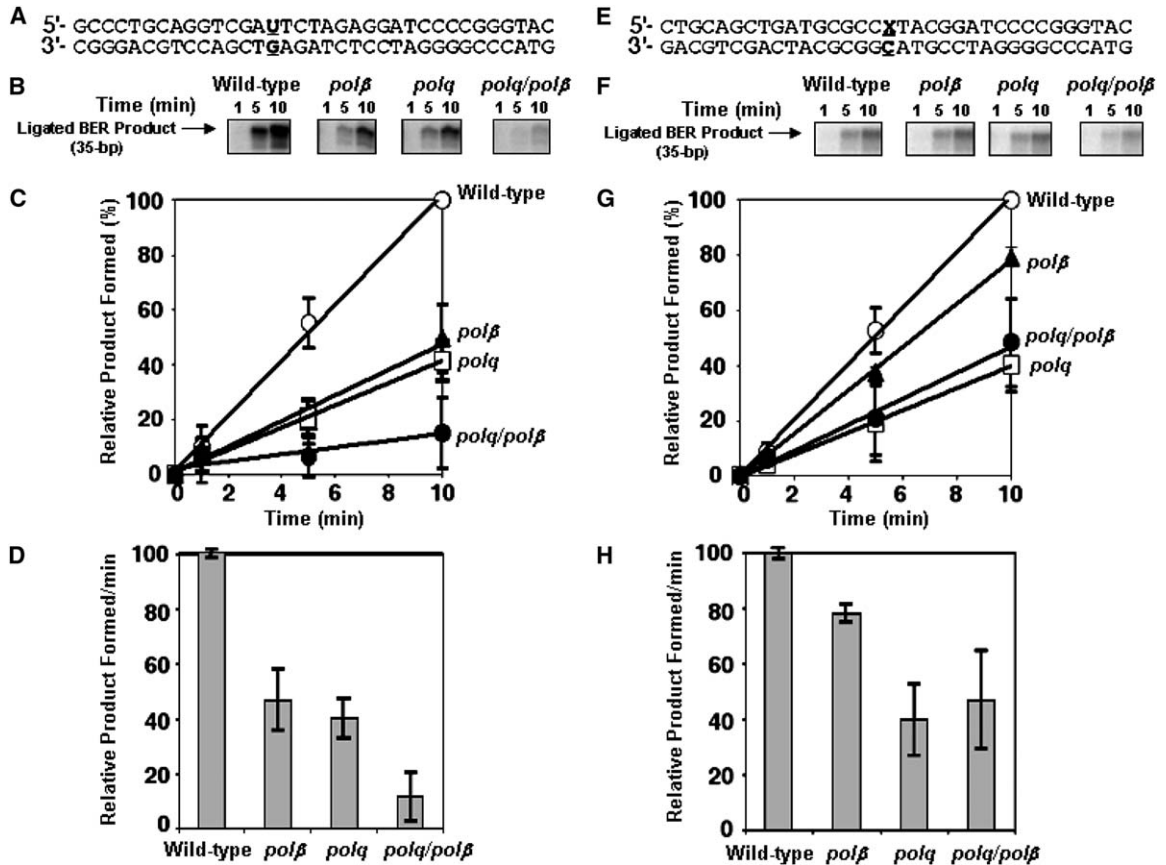


Figure 3. Kinetic Analysis of In Vitro BER in Cellular Extract

DNA synthesis on a BER substrate containing either uracil (A–D) or 8-oxoG (E–H) oligonucleotides was evaluated by measuring the incorporation of [α - 32 P]dCMP or [α - 32 P]dGMP with time using DT40 cell extracts.

(A) A line diagram of a 35 bp oligonucleotide containing a uracil residue at position 15 is illustrated.

(B) The in vitro BER capacity of the indicated cell extracts. Whole-cell extract (10 μ g) was incubated with DNA (50 nM) at 37°C, and aliquots were withdrawn at different time intervals. The reaction products were separated by 15% denaturing polyacrylamide gel electrophoresis, and the gels were scanned by a phosphorimager to quantify ligated BER products (35 bp).

(C) The experiment shown in (B) was repeated three times, and average values of the repair product were plotted. The amount of product formed in 10 min reaction using wild-type cell extract was set to 100% in each experiment. The averages of relative percent of repair product (%), Y axis) were plotted against incubation time (min, X axis). Error bars show the SD of the mean for three independent experiments.

(D) The average initial rate of BER reaction in the indicated cellular extract is shown in a bar diagram. Initial rates were calculated by applying a curve fit program to the data shown in (C). Error bars show the SD of the mean for three independent experiments.

(E) A line diagram of a 34 bp oligonucleotide containing an 8-oxoG (X) residue at position 17 is illustrated.

(F–H) Data in (F)–(H) are presented as in (B)–(D), respectively. (G and H) Error bars show the SD of the mean for three independent experiments.

gaps with time after DNA damage, because such BER intermediate products are eliminated by the action of DNA polymerases. To this end, we employed a real-time assay to monitor intracellular NAD(P)H during continuous exposure to MMS and HmdUrd and following pulse exposure of cells to H₂O₂. This assay is extremely sensitive, because single-strand discontinuities quickly and continuously activate poly[ADP-ribose]polymerase (PARP) (Okano et al., 2003), reducing the level of the intracellular NAD(P)H (the source of ADP-ribose for PARP) until the SSBs are repaired. Accordingly, the extent of intracellular NAD(P)H depletion may reflect the number of unrepaired SSBs and gaps (Nakamura et al., 2003) and thus may be inversely correlated with the activity of the DNA polymerases that fill these lesions. To test whether or not the NAD(P)H depletion is detectable only in BER-deficient cells, we measured the level of NAD(P)H during continuous exposure to HmdUrd. As

a negative control, we chose *polζ* cells, which are deficient in TLS, but not in BER, and are sensitive to a variety of DNA-damaging agents including UV, γ rays, MMS, H₂O₂, and chemical crosslinking agents (Okada et al., 2005; Sonoda et al., 2003). Both *polζ* and *polβ* cells were sensitive to HmdUrd (Figure 2G). POL ζ is likely to be involved in bypassing abasic sites (Gibbs et al., 2005), which are generated as intermediates in BER of incorporated HmdUrd. As expected, *polβ* cells, but not *polζ* cells, exhibited more significant NAD(P)H depletion compared to wild-type cells during continuous exposure to HmdUrd (Figures 5A and 5D). Furthermore, *polζ* and wild-type cells were indistinguishable in the level of NAD(P)H depletion during continuous exposure to MMS and after pulse exposure to H₂O₂ (Figures 5B, 5C, 5E, and 5F). These results confirm that the level of intracellular NAD(P)H is not affected by defects in TLS, but rather reflects BER intermediates.

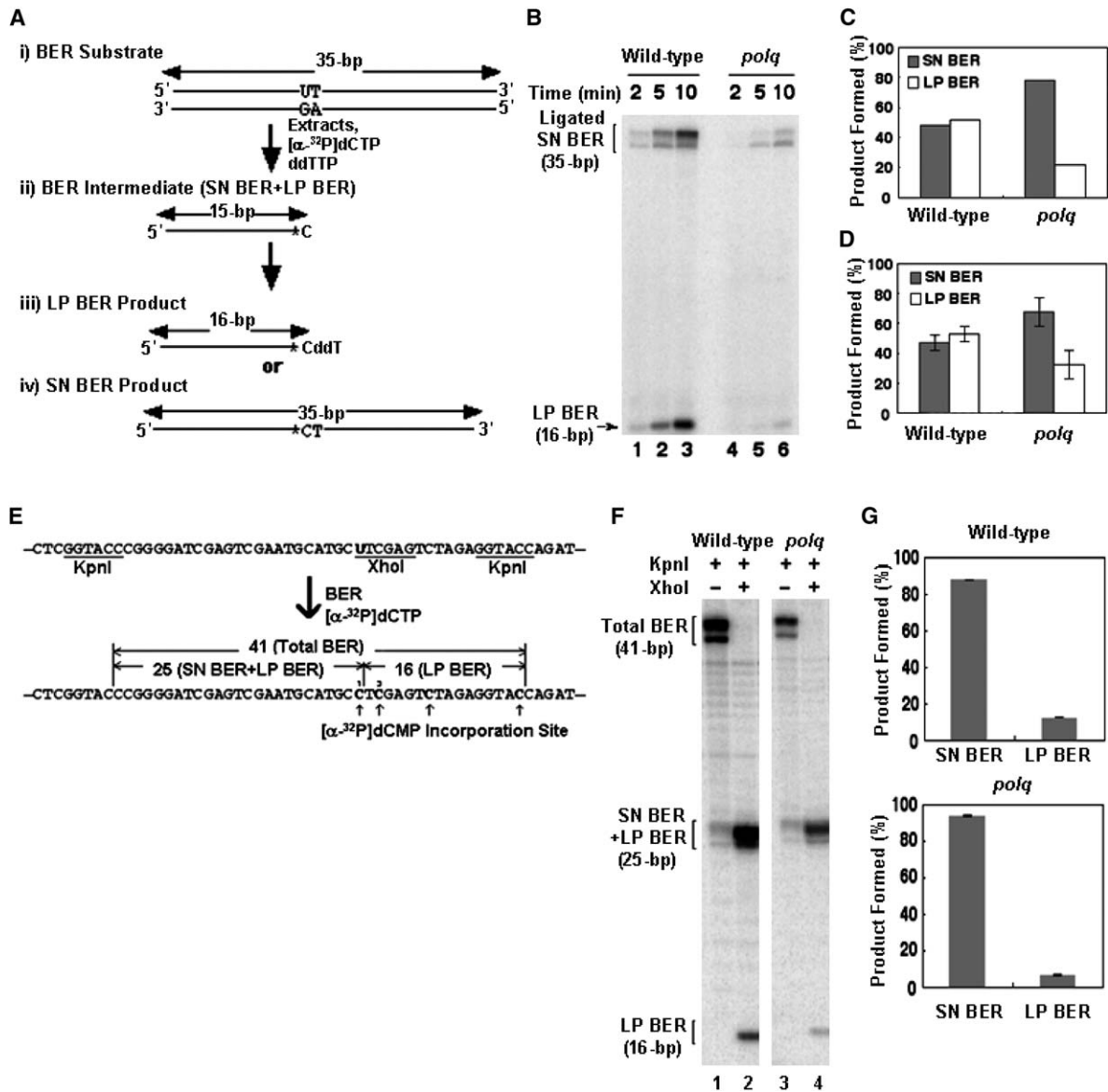


Figure 4. Contribution of POLQ to LP as Well as SN BER of Uracil-containing Oligonucleotide DNA

The activity of SN BER and LP BER was differentially measured in vitro using oligonucleotide substrate (A–D) or plasmid substrate (E–G). (A) A schematic representation of the substrate DNA and predicated BER reaction products and intermediates is shown. Incorporation of [α - 32 P]dCMP was measured in the presence of ddTTP to discriminate between SN BER and LP BER. The incubations were performed with wild-type and *polq* null DT40 cell extracts at different time intervals, and the reaction products were separated by 15% denaturing polyacrylamide gel electrophoresis. The reaction products were analyzed differentially for SN BER and LP BER. (i) BER substrate: the same uracil-containing oligonucleotide as in Figure 3A was utilized. (ii–iv) The sizes and intermediates of BER are as follows: 1 nt addition representing SN plus LP BER (15 bp), 16 nt product representing LP BER only, and 35 nt product generated by SN BER followed by ligation with the downstream strand. [α - 32 P]dCMP was incorporated in the position of uracil (marked by *C) in both SN and LP BER. The “ddT” designates incorporation of ddTTP. Note that the incorporation of ddTTP followed by [α - 32 P]dCMP in LP BER prevents further extension of repair DNA synthesis. (B) A representative autoradiograph of gel electrophoresis to measure in vitro BER products following the indicated incubation time. The in vitro BER was performed with cell extracts isolated from wild-type (lanes 1–3) and *polq* mutant (lanes 4–6) cells. (C) The ratio of SN BER and LP BER in wild-type and *polq* mutant cell extracts for 10 min ([B], lanes 3 and 6) is shown. (D) The average values and standard deviations of SN BER (gray) and LP BER (white) in 10 min reactions from three independent experiments are shown. (E) A schematic representation of the uracil-containing plasmid DNA substrate, the strategic restriction sites, and the predicated SN BER and LP BER products is shown. Plasmid DNA contained a solitary uracil residue (in bold), and KpnI and XhoI restriction-enzyme sites (underlined). After incubation of the plasmid with DT40 cell extracts in the presence of [α - 32 P]dCTP for 30 min at 37°C, the repair products were digested by KpnI or a mixture of KpnI and XhoI, and the radioactivity in each digested fragment was measured. The replacement of uracil by [32 P]dCMP (the first C) and subsequent ligation with the downstream strand may result in 32 P labeling of the 25 bp KpnI-XhoI fragment (representing SN BER plus LP BER), whereas incorporation of 32 P-dCMP at position 3 and beyond may result in 32 P labeling of the 16 bp XhoI-KpnI fragment (representing LP BER). (F) A representative autoradiograph of reaction products separated by 15% denaturing polyacrylamide gel electrophoresis. (G) The ratio of SN BER and LP BER in wild-type (top) and *polq* mutant (bottom) cell extracts. The amount of the SN BER product was calculated by subtracting the radioactivity of the 16 bp fragment (LP BER product) from that of the 25 bp fragment. Note that the incorporation of 32 P at 8th and

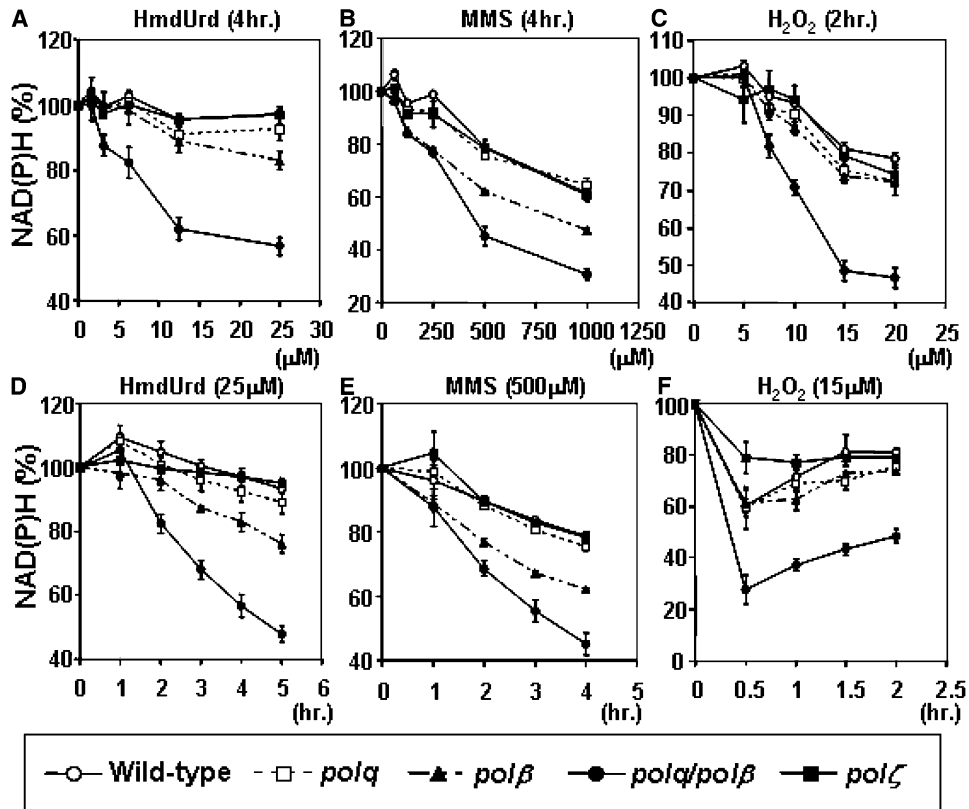


Figure 5. Monitoring the Level of Unrepaired SSBs by Measuring Intracellular NAD(P)H Concentrations

The relationship between intracellular level of NAD(P)H and dose of damaging agents is shown. Cells were continuously exposed to HmdUrd and MMS at different concentrations for 4 hr and exposed to H₂O₂ at different concentrations for 30 min followed by 1.5 hr repair period (A–C). The kinetics of intracellular NAD(P)H depletion during continuous exposure of cells to 25 μM HmdUrd and 500 μM MMS, as shown in (D)–(E). The kinetics of intracellular NAD(P)H depletion in cells treated with 15 μM H₂O₂ for 30 min followed by up to 1.5 hr repair period, as shown in (F). Mean and SD (bars) are from triplicate cultures in triplicate experiments.

We used this assay to compare the BER capacity of *polq*, *pol β* , and *polq/pol β* cells (Figure 5). During continuous exposure to MMS and HmdUrd, the NAD(P)H levels in *polq* and wild-type cells were indistinguishable, whereas *pol β* single mutants showed a moderate increase in the level of depletion. However, a significant increase in PARP activity was detectable in *polq/pol β* cells as judged by NAD(P)H depletion (Figures 5A, 5B, 5D, and 5E). This observation correlates well with the observed increase in sensitivity in the double mutant (Figures 2E and 2G).

The sensitivity of *polq* cells to H₂O₂ (Figure 2F) implies a defect in BER and/or TLS past oxidative damage. In contrast with cellular response to MMS or HmdUrd, there is a discrepancy between colony survival (Figure 2F) and NAD(P)H depletion after H₂O₂ treatment (Figures 5C and 5F), because *polq* cells displayed reduced survival but showed no increase in NAD(P)H depletion when compared with wild-type cells. Thus, in the case of H₂O₂, *polq* cells resemble more closely *pol ζ* cells, which are hypersensitive to a variety of DNA damage without showing depletion of NAD(P)H. We therefore postulate that the increased H₂O₂ sensitivity of single *polq* mutant cells may be caused by defective

TLS, rather than by defective BER, as suggested recently by Seki et al. (Seki et al., 2004). On the other hand, defects in *polq/pol β* double mutants revealed a synergistic effect on depletion of NAD(P)H after H₂O₂ (Figures 5C and 5F). Thus, POLQ also has a function redundant with POL β in BER of H₂O₂-induced damage. The role for POLQ in BER of oxidative damage is supported by the in vitro BER of 8-oxoG (Figures 3G and 3H). These data suggest that POLQ and POL β have overlapping roles in BER of a variety of DNA lesions.

Rapid Recruitment of POLQ to DNA Lesions

Our findings of a reduction in BER activity in *polq/pol β* cells led us to assess the general relevance of the data from DT40 cells by analyzing POLQ localization to base damage in mammalian cells. We investigated the localization pattern of green fluorescent protein (GFP)-tagged human POLQ in living cells with time after inducing base damage in a subnuclear area by UVA laser (Lan et al., 2004). SSBs, double-strand breaks, and base damage can be generated by exposing cells to 405 nm laser irradiation (Lan et al., 2005). In this assay, association of a repair factor with either SSBs or base damage can be distinguished, because higher doses of irradiation

17th of C (shown by arrows) by LP BER occurred only occasionally (see Experimental Procedures). The experiments were repeated three times. The average values and standard deviations are shown in a bar diagram.

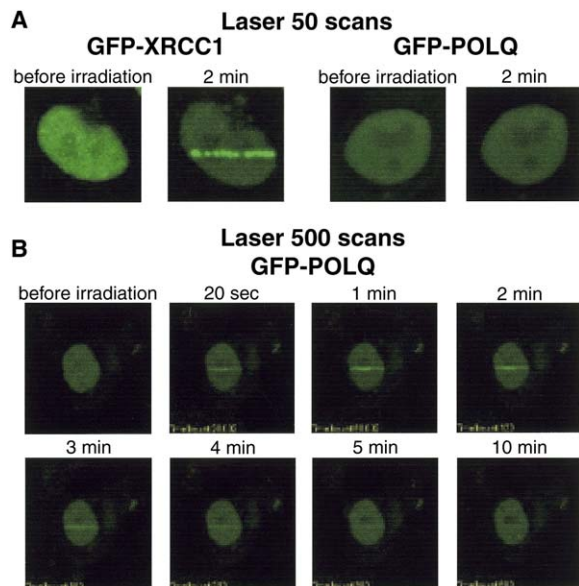


Figure 6. Transient Accumulation of POLQ at Sites of Base Damage Induced by UV Laser Irradiation

(A) HeLa cells transiently expressing GFP-XRCC1 or GFP-POLQ were irradiated with 405 nm laser light (50 scans). GFP signals before irradiation and 2 min after irradiation are shown.

(B) Accumulation of GFP-POLQ after 500 scans of 405 nm laser irradiation.

(500 scans of irradiation) are required for the induction of base damage, while only 50 scans of laser irradiation is sufficient for generation of SSBs. Accordingly, GFP-tagged XRCC1, which is involved in both SSB repair and BER, accumulated at the irradiated site at 2 min following 50 scans of irradiation (Figure 6A, left). However, the accumulation of GFP-tagged POLQ was undetectable following 50 scans (Figure 6A, right) but was observed after 500 scans of irradiation (Figure 6B). The accumulation reached a peak around 2 min, decreased rapidly, and disappeared 10 min after irradiation (Figure 6B). These kinetics of accumulation and dissociation of POLQ are similar to those of POL β in *xrcc1*-deficient cells (Lan et al., 2004). Taken together, genetic, biochemical, and cell biological analysis points to an important role for POLQ in the BER pathway.

Discussion

In this report, we propose a new function for vertebrate POLQ. The phenotype we observe in DT40 *polq* mutants is essentially different from the one observed in *Drosophila mus308* mutants. Vertebrate POLQ paralog proteins do not appear to be involved in the repair of chemical crosslinking agents, as the phenotype of POLQ-deficient mice would also suggest (Shima et al., 2004). Conversely, we found that vertebrate POLQ plays an important role in BER, most likely at the repair synthesis step.

Although *polq* cells showed no significant increase in sensitivities to MMS or HmdUrd, *polq/pol β* cells were more sensitive to these agents than were the single mutants. A simple interpretation of these data is that the two polymerases share a function in which POL β is preferentially used over POLQ. A role for these polymer-

ases in BER is indicated by in vitro BER assays (Figures 3 and 4) and real-time NAD(P)H measurements to assess the level of unfilled single-strand gaps in the cells (Figure 5). Although *polq* cells showed no increased sensitivity to MMS or HmdUrd in the colony-survival assay (Figure 2), the in vitro BER activity of *polq* cellular extract was significantly reduced compared to that of wild-type cellular extract (Figure 3). This discrepancy between the colony-survival data and in vitro BER efficacy might be explained by the idea that the DNA synthesis step in BER in vivo is not necessarily a rate-limiting step if either POL β or POLQ is present. Moreover, the MMS hypersensitivity of *pol β* cells is caused by defective elimination of 5' deoxyribose phosphate as well as loss of polymerase activity (Sobol et al., 2000).

Regarding the kinetics of NAD(P)H depletion following damage induction, a defect in POLQ had an impact only in the absence of POL β . In summary, the observed hypersensitivity in *polq/pol β* cells and a severe NAD(P)H depletion in *polq/pol β* cells in response to these agents suggest that POLQ plays a role in the BER pathway and backs up the BER functions of POL β . Moreover, POLQ accumulated at laser-induced base damage immediately after irradiation of human cells and reached a peak in accumulation around 2 min after irradiation. This pattern of rapid accumulation is reminiscent of other BER factors, such as POL β , which peaks at the break around 2.5 min after damage induction (Lan et al., 2004). In summary, we provide evidence for a role for POLQ in BER by genetic, biochemical, and cell biological means in both DT40 and human cells.

A defect in BER in *polq* cells may lead to more frequent blocks in DNA replication at sites of endogenous DNA damage, leading to spontaneously arising chromosomal breaks, as shown in mice carrying mutations or deletions of POLQ (Shima et al., 2003, 2004). It may also lead to more frequent usage of homologous recombination-mediated repair, as evidenced by an increase in the level of spontaneous SCE. Similarly, a defect in TLS in *polq* cells may result in increased levels of chromosomal breaks and SCE during the cell cycle. Thus, POLQ appears to contribute to the maintenance of chromosomal DNA by functioning in both BER and TLS. A role for POLQ in two pathways of DNA damage tolerance is reminiscent of the dual function suggested for POL κ in both nucleotide excision repair and TLS (Ogi and Lehmann, 2006), and the dual function of POL η in both homologous DNA recombination and TLS (Kawamoto et al., 2005).

Experimental Procedures

Cloning of the Chicken POLQ, HEL308, and POLN Genes

A chicken full-length cDNA of POLQ and partial cDNAs of HEL308 and POLN were isolated by RT-PCR from chicken testis cDNA. Primers were designed according to the information of BBSRC chicken EST database (<http://www.chick.umist.ac.uk/>). A full-length sequence of GdHEL308 and partial GdPOLN sequence were isolated by 5'- and 3'-RACE.

Constructing of Targeting Vectors

The positions of exons and introns were determined by base sequencing. Two POLQ disruption constructs of the helicase domain, POLQ-*hisD* and POLQ-*bsr*, were generated from genomic PCR products combined with *hisD* and *bsr* selection marker cassettes, and two POLQ disruption constructs of the polymerase domain, POLQ-*neo* and POLQ-*puro*, were generated from genomic PCR

products combined with puro and neo selection marker cassettes flanked by *loxP*. Genomic DNA sequences were amplified using the primers 5'-CTGGAAGGGCTGGCAGGAAAGGAG-3' and 5'-TCTAAGCAAACTGCGAACAGGC-3' (for the left arm of the KO construct of the helicase domain) and 5'-GGGAGATCTGAAATATCACAGTCTGGGA-3' and 5'-ATGATTACGCCAAGCTTGGTACCG-3' (for the right arm of the KO construct of the helicase domain). Amplified PCR products (1.5 kb for the left arm, 6 kb for the right arm) were cloned into pCR2.1-TOPO vector (Invitrogen). The 1.5 kb fragment (BamHI/BglII) from the left arm was cloned into the BamHI site of the pCR2.1 containing 6 kb right arm sequence. The BamHI site was used to clone marker gene cassettes. The 1.0 kb fragment from the genomic DNA amplified using the primers 5'-AGCGATTCAGCCCGCTAGAATGCTC-3' and 5'-CAACAGTGTTCACAAGCAGGAG-3' was used as a probe for Southern blot analysis. Genomic DNA sequences were amplified using the primers 5'-GCCACAGTTTCTCCTTGACCAGCTC-3' and 5'-GCACATTCTGGATATTTGGCTCTGCG-3' (for the left arm of the KO construct of the polymerase domain) and 5'-GGGGATCCCCATACCCATCTTTCTGCA-3' and 5'-CCGCATGGAGCCAGCCTGTCCTG-3' (for the right arm of the KO construct of the polymerase domain). Amplified PCR products (4.5 kb for the left arm, 2.5 kb for the right arm) were cloned into pCR2.1-TOPO vector. The 2.5 kb fragment (BamHI/BglII) from the left arm was cloned into the BamHI site of the pCR2.1 containing 4.5 kb left arm sequence. The BamHI site was used to clone marker gene cassettes. The 0.8 kb fragment from the genomic DNA amplified using the primers 5'-GGTCCAGGACAGCTATTTACTGTGG-3' and 5'-CTTGCTGCTGCTGCTGGTGTCTG-3' was used as a probe for Southern blot analysis. Two *HEL308* disruption constructs, *HEL308-puro* and *HEL308-neo*, were generated from genomic PCR products combined with puro and neo selection marker cassettes flanked by *loxP*. Genomic DNA sequences were amplified using the primers 5'-ATCGGTGTCATCATCTCCGTGTCCTG-3' and 5'-TTCCACCACTAGTTGGTAACGAG-3' (for the left arm of the KO construct) and 5'-TGATTGGCAGAGCTGGTCGAGCTGGG-3' and 5'-TTCTGATGGCTTGACCAGAGGCT-3' (for the right arm of the KO construct). Amplified PCR products (0.9 kb for the left arm, 5 kb for the right arm) were cloned into pCR2.1-TOPO vector. The 0.9 kb EcoRI fragment (blunt ended) from the left arm was cloned into the HindIII site (blunt ended) of the pCR2.1 containing 5 kb right arm sequence. The BamHI site was used to clone marker gene cassettes. The 0.6 kb EcoRI fragment from the genomic DNA amplified using the primers 5'-ATCAGCTCCGCTCGCAAACGGAGCC-3' and 5'-TCCAGTGCTTTCACGTCCAGGCCT-3' was used as a probe for Southern blot analysis. Two *POLN* disruption constructs, *POLN-hisD* and *POLN-bsr*, were generated from genomic PCR products combined with *hisD* and *bsr* selection marker cassettes flanked by *loxP*. Genomic DNA sequences were amplified using the primers 5'-GGCTGATAAACTCCAGCGACACGGTTCC-3' and 5'-CCGTCCACATAGGTTGATTTTCATCTTCC-3' (for the left arm of the KO construct) and 5'-GGGGATCCACAGCAAGTTCATCCACCTC-3' and 5'-GGCAAAGGATGAAGATCTTGCAACTTACC-3' (for the right arm of the KO construct). Amplified PCR products (4.5 kb for the left arm, 1.3 kb for the right arm) were cloned into pCR2.1-TOPO vector. The pCR2.1-TOPO vector was digested by *SpeI* and then ligated. The 1.3 kb fragment (BamHI/BglII) from the right arm was cloned into the BamHI site of the pCR2.1 containing 4.5 kb left arm sequence. The BamHI site was used to clone marker gene cassettes. The 0.3 kb fragment from the genomic DNA amplified using the primers 5'-CGGAAGATGAAATCAACCTATGTGGACGG-3' and 5'-GTCACAGTTCCTGTCTGATTCCATGTAGGG-3' was used as a probe for Southern blot analysis. Linearization of the plasmids was done prior to transfection into DT40 cells; *POLQ-bsr* and *POLQ-hisD* were digested with *XhoI*, and *POLQ-neo* and *POLQ-puro* were digested with *KpnI*; *HEL308-puro*, *HEL308-neo*, *POLN-hisD*, and *POLN-bsr* were digested with *NotI*.

Transfection and Cell Culture

The conditions for cell culture, selection, and DNA transfections have been described previously (Sonoda et al., 2003).

Colony-Formation Assay

Colony-formation assay was performed as described previously (Okada et al., 2005), with the following modification in exposure to

MMC and HmdUrd. To analyze sensitivities to MMC (Kyowa Hakko, Japan), and HmdUrd (Sigma), 1×10^5 cells were treated at 39.5°C in 1 ml of the complete medium containing pertinent concentration of MMC and HmdUrd for 1 hr.

The Preparation of Oligonucleotide Substrates and Cellular Extract for In Vitro BER Assay

The DNA substrate for the uracil-initiated BER assay was a 35 bp duplex DNA constructed by annealing two synthetic oligodeoxyribonucleotides (Oligos Etc.) to introduce a G:U base pair at position 15: 5'-GCCCTGCAGGTCGAUTCTAGAGGATCCCCGGGTAC-3' and 5'-GTACCCGGGGATCCTCTAGAGTCGACCTGCAGGGC-3'. Gel-purified synthetic 34 bp oligodeoxyribonucleotides containing an 8-oxoG:C mismatch at position 17 were obtained from Operon Technologies (Alameda, California): 5'-CTGCAGCTGATCGCC\8-oxoG\TACGGATCCCCGGGTAC-3' and 5'-GTACCCGGGGATCCGTACGGCGCATCAGCTGCAG-3'. Cell extracts were prepared as previously described (Biade et al., 1998). Briefly, cells were collected by centrifugation and resuspended in buffer 1 (10 mM Tris-HCl [pH 7.8], 200 mM KCl, and protease inhibitor cocktail) (Boehringer Mannheim). An equal volume of buffer 2 (10 mM Tris-HCl [pH 7.8], 200 mM KCl, 2 mM EDTA, 40% glycerol, 0.2% Nonidet P-40, 2 mM DTT, and protease inhibitor cocktail) was added. The resulting extract was clarified by centrifugation at 14,000 rpm at 4°C for use in in vitro BER assays.

In Vitro BER Assay Using Oligonucleotide Substrate

The BER reaction (final volume of 10 μ l) was performed with a 35 bp oligonucleotide DNA substrate containing uracil at position 15 or a 34 bp oligonucleotide DNA substrate containing 8-oxoG at position 17. The duplex oligonucleotide substrate at a final concentration of 50 nM was incubated with 10 μ g of DT40 whole-cell extract in 50 mM Tris-HCl (pH 7.5), 5 mM MgCl₂, 20 mM NaCl, 0.5 mM DTT, and 4 mM ATP; for the uracil-mediated BER assay, the incubation was conducted in the presence of 20 μ M each dATP, dGTP, and dTTP, and 2.3 μ M [α -³²P]dCTP at 37°C for 1, 5, and 10 min; for the 8-oxoG-mediated BER assay, the incubation was conducted using 20 μ M each dATP, dCTP, and dTTP, and 2.3 μ M [α -³²P]dGTP. For the uracil-mediated oligonucleotide-based LP BER assay, the incubation was conducted in the presence of 2.3 μ M [α -³²P]dCTP and 50 μ M ddTTP at 37°C for 2, 5, and 10 min, as described previously (Harrigan et al., 2006). The reaction products were analyzed by 15% denaturing polyacrylamide gel electrophoresis. The initial rates of the in vitro BER reactions were determined by plotting the arbitrary phosphorimager units of ligated BER products against each time point.

In Vitro BER Assay Using Plasmid Substrate

Uracil-containing plasmid DNA was designed to discriminate total BER, SN BER, and LP BER, as described by Hou et al. (E.H., R.P., K.A., and S.H.W., unpublished data). The 41 nucleotide *KpnI* fragment containing uracil (see Figure 4E) was ligated with *KpnI*-digested pBS vector. BER reaction mixture (final volume of 10 μ l) contained 20 nM plasmid DNA, 10 μ g of DT40 whole-cell extract prepared from wild-type or *polq* cells, 50 mM Tris-HCl (pH 7.5), 5 mM MgCl₂, 20 mM NaCl, 1 mM DTT, 4 mM ATP, 20 μ M each dATP, dGTP, and dTTP, and 2.3 μ M [α -³²P]dCTP. The incubation was conducted at 37°C for 30 min. After phenol/chloroform extraction and ethanol precipitation, the recovered reaction product was subjected to the restriction-enzyme analysis. The resulting reaction products were separated by 15% denaturing polyacrylamide gel electrophoresis. The plasmid is designed to detect total BER product (41 bp *KpnI* fragment), SN BER plus LP BER (25 bp *KpnI*-*XhoI* fragment), and LP BER (16 bp *XhoI*-*KpnI* fragment). Gels were scanned by phosphorimager, and the reaction products were quantified by ImageQuant software. For the calculation of SN BER, arbitrary phosphorimager units in the 16 bp fragment were subtracted from that of 25 bp fragment. The experiments were repeated three times, and the average values of SN BER and LP BER were plotted in the form of a histogram. The in vitro BER using either [α -³²P]dCTP or [α -³²P]dTTP showed that incorporation of T did not exceed that of C in the 16 nt fragment, indicating that the vast majority of repair synthesis was less than seven nucleotides, and, thus, the incorporation of ³²P-labeled CMP at the 8th to 17th nucleotides (shown by arrows in Figure 4E) by LP BER was negligible. Thus, the radioactivity of

both 16 and 25 nt fragments should reflect single ^{32}P incorporation per fragment.

Monitoring Intracellular NAD(P)H

SSB repair capacity was determined by monitoring intracellular NAD(P)H levels using a real-time, colorimetric assay. NAD(P)H depletion served as a surrogate for NAD⁺ consumption from PARP1 activation, a requisite step in SSB repair (Nakamura et al., 2003). For cells continuously exposed to MMS (Aldrich) or HmdUrd (Sigma), NAD(P)H levels were monitored using a redox dye mixture consisting of XTT (Sigma) and 1-methoxy PMS (Sigma) as described by Takanami et al. (Takanami et al., 2005). For H₂O₂ exposure, cells were first incubated with H₂O₂ for 30 min with the subsequent addition of complete medium, dye mixture, and catalase (Sigma, 36 units/ml) for the monitoring of intracellular NAD(P)H.

Laser Assay

The cDNA of human *POLQ* was cloned into the BglIII/SmaI site of pEGFP-C2 vector (Clontech). GFP was fused at the N terminus of *POLQ*. HeLa cells were propagated in DMEM (Nissui) supplemented with 10% fetal bovine serum at 37°C and 5% CO₂. Cells were plated on glass-bottom dishes (Matsunami Glass) at 50% confluence 24 hr before the transfection (Fugene-6, Life Technology) and irradiated with laser light under a microscope 48 hr after transfection. Fluorescence images were obtained and processed using a FV-500 confocal scanning laser microscopy system (Olympus). We used a 405 nm scan laser system (Olympus) for irradiation of cells in the epifluorescence path of the microscope system. The power of the scan laser can be controlled by scanning times or by laser power. By using this system, various types of DNA damage, such as SSBs (produced by lower dose and higher dose irradiation) and double-strand breaks and oxidative base damage (produced by higher dose irradiation), were produced at restricted nuclear regions of mammalian cells. One scan of the laser light at full power delivers energy of around 1600 nW. We used only full power from the 405 nm laser in this study and regulated the dose by changing the scanning times. Laser light was focused through a 40× objective lens. Cells were incubated with Opti-medium (GIBCO) in glass-bottom dishes, which were placed in chambers to prevent evaporation, on a 37°C hot plate. The energy of fluorescent light at the irradiated site was measured with a laser power/energy monitor (ORION, Ophir Optonics).

Analysis of Chromosome Aberrations and SCE Events

Measurement of chromosome aberrations and SCE levels was performed as described previously (Sonoda et al., 2003). To induce SCE, cells were incubated with 10 μM H₂O₂ for 18 hr.

Supplemental Data

Supplemental Data include three figures and Supplemental Experimental Procedures and can be found with this article online at <http://www.molecule.org/cgi/content/full/24/1/115/DC1/>.

Acknowledgments

We would like to thank H. Onisawa, Y. Murakawa, A. Ohno, and S. Torikoshi for their technical assistance. We also acknowledge Drs. A. Lehmann, K. Caldecott, and C. Breslin for critical reading and suggestion. Financial support was provided in part by grant of Core Research for Evolutional Science and Technology (CREST) from Japan Science and Technology Corporation, by the Center of Excellence (COE) grant for Scientific Research from the Ministry of Education, Culture, Sports, Science and Technology of the Japanese government, by grants from The Uehara Memorial Foundation and The Naito Foundation, by NIEHS grant P30-ES10126 to J.N., and by NIH grant CA101980 to R.D.W. This research was also supported in part by the Intramural Research Program of the NIH.

Received: March 6, 2006

Revised: July 2, 2006

Accepted: July 28, 2006

Published: October 5, 2006

References

- Barnes, D.E., and Lindahl, T. (2004). Repair and genetic consequences of endogenous DNA base damage in mammalian cells. *Annu. Rev. Genet.* 38, 445–476.
- Biade, S., Sobol, R.W., Wilson, S.H., and Matsumoto, Y. (1998). Impairment of proliferating cell nuclear antigen-dependent apurinic/aprimidinic site repair on linear DNA. *J. Biol. Chem.* 273, 898–902.
- Boyd, J.B., Sakaguchi, K., and Harris, P.V. (1990). *mus308* mutants of *Drosophila* exhibit hypersensitivity to DNA cross-linking agents and are defective in a deoxyribonuclease. *Genetics* 125, 813–819.
- Braithwaite, E.K., Prasad, R., Shock, D.D., Hou, E.W., Beard, W.A., and Wilson, S.H. (2005). DNA polymerase lambda mediates a back-up base excision repair activity in extracts of mouse embryonic fibroblasts. *J. Biol. Chem.* 280, 18469–18475.
- Gibbs, P.E., McDonald, J., Woodgate, R., and Lawrence, C.W. (2005). The relative roles in vivo of *Saccharomyces cerevisiae* Pol eta, Pol zeta, Rev1 protein and Pol32 in the bypass and mutation induction of an abasic site, T-T (6-4) photoadduct and T-T cis-syn cyclobutane dimer. *Genetics* 169, 575–582.
- Harrigan, J.A., Wilson, D.M., III, Prasad, R., Opresko, P.L., Beck, G., May, A., Wilson, S.H., and Bohr, V.A. (2006). The Werner syndrome protein operates in base excision repair and cooperates with DNA polymerase beta. *Nucleic Acids Res.* 34, 745–754.
- Hohegger, H., Sonoda, E., and Takeda, S. (2004). Post-replication repair in DT40 cells: translesion polymerases versus recombinases. *Bioessays* 26, 151–158.
- Izumi, T., Brown, D.B., Naidu, C.V., Bhakat, K.K., Macinnes, M.A., Saito, H., Chen, D.J., and Mitra, S. (2005). Two essential but distinct functions of the mammalian abasic endonuclease. *Proc. Natl. Acad. Sci. USA* 102, 5739–5743.
- Kawamoto, T., Araki, K., Sonoda, E., Yamashita, Y.M., Harada, K., Kikuchi, K., Masutani, C., Hanaoka, F., Nozaki, K., Hashimoto, N., and Takeda, S. (2005). Dual roles for DNA polymerase eta in homologous DNA recombination and translesion DNA synthesis. *Mol. Cell* 20, 793–799.
- Lan, L., Nakajima, S., Oohata, Y., Takao, M., Okano, S., Masutani, M., Wilson, S.H., and Yasui, A. (2004). In situ analysis of repair processes for oxidative DNA damage in mammalian cells. *Proc. Natl. Acad. Sci. USA* 101, 13738–13743.
- Lan, L., Nakajima, S., Komatsu, K., Nussenzweig, A., Shimamoto, A., Oshima, J., and Yasui, A. (2005). Accumulation of Werner protein at DNA double-strand breaks in human cells. *J. Cell Sci.* 118, 4153–4162.
- Lindahl, T. (1993). Instability and decay of the primary structure of DNA. *Nature* 362, 709–715.
- Lindahl, T. (2000). Suppression of spontaneous mutagenesis in human cells by DNA base excision-repair. *Mutat. Res.* 462, 129–135.
- Marini, F., and Wood, R.D. (2002). A human DNA helicase homologous to the DNA cross-link sensitivity protein Mus308. *J. Biol. Chem.* 277, 8716–8723.
- Marini, F., Kim, N., Schuffert, A., and Wood, R.D. (2003). POLN, a nuclear PolA family DNA polymerase homologous to the DNA cross-link sensitivity protein Mus308. *J. Biol. Chem.* 278, 32014–32019.
- Masuda, K., Ouchida, R., Takeuchi, A., Saito, T., Koseki, H., Kawamura, K., Tagawa, M., Tokuhisa, T., Azuma, T., and O-Wang, J. (2005). DNA polymerase theta contributes to the generation of C/G mutations during somatic hypermutation of Ig genes. *Proc. Natl. Acad. Sci. USA* 102, 13986–13991. Published online September 19, 2005. 10.1073/pnas.0505636102.
- Matsubara, M., Tanaka, T., Terato, H., Ohmae, E., Izumi, S., Katayanagi, K., and Ide, H. (2004). Mutational analysis of the damage-recognition and catalytic mechanism of human SMUG1 DNA glycosylase. *Nucleic Acids Res.* 32, 5291–5302.
- Nakamura, J., La, D.K., and Swenberg, J.A. (2000). 5'-nicked apurinic/aprimidinic sites are resistant to beta-elimination by beta-polymerase and are persistent in human cultured cells after oxidative stress. *J. Biol. Chem.* 275, 5323–5328.
- Nakamura, J., Asakura, S., Hester, S.D., de Murcia, G., Caldecott, K.W., and Swenberg, J.A. (2003). Quantitation of intracellular

NAD(P)H can monitor an imbalance of DNA single strand break repair in base excision repair deficient cells in real time. *Nucleic Acids Res.* **31**, e104.

Ogi, T., and Lehmann, A.R. (2006). The Y-family DNA polymerase kappa (pol kappa) functions in mammalian nucleotide-excision repair. *Nat. Cell Biol.* **8**, 640–642.

Okada, T., Sonoda, E., Yoshimura, M., Kawano, Y., Saya, H., Kohzaki, M., and Takeda, S. (2005). Multiple roles of vertebrate REV genes in DNA repair and recombination. *Mol. Cell. Biol.* **25**, 6103–6111.

Okano, S., Lan, L., Caldecott, K.W., Mori, T., and Yasui, A. (2003). Spatial and temporal cellular responses to single-strand breaks in human cells. *Mol. Cell. Biol.* **23**, 3974–3981.

Seki, M., Marini, F., and Wood, R.D. (2003). POLQ (Pol theta), a DNA polymerase and DNA-dependent ATPase in human cells. *Nucleic Acids Res.* **31**, 6117–6126.

Seki, M., Masutani, C., Yang, L.W., Schuffert, A., Iwai, S., Bahar, I., and Wood, R.D. (2004). High-efficiency bypass of DNA damage by human DNA polymerase Q. *EMBO J.* **23**, 4484–4494.

Shima, N., Hartford, S.A., Duffy, T., Wilson, L.A., Schimenti, K.J., and Schimenti, J.C. (2003). Phenotype-based identification of mouse chromosome instability mutants. *Genetics* **163**, 1031–1040.

Shima, N., Munroe, R.J., and Schimenti, J.C. (2004). The mouse genomic instability mutation chaos1 is an allele of Polq that exhibits genetic interaction with Atm. *Mol. Cell. Biol.* **24**, 10381–10389.

Sobol, R.W., Horton, J.K., Kuhn, R., Gu, H., Singhal, R.K., Prasad, R., Rajewsky, K., and Wilson, S.H. (1996). Requirement of mammalian DNA polymerase-beta in base-excision repair. *Nature* **379**, 183–186.

Sobol, R.W., Prasad, R., Evenski, A., Baker, A., Yang, X.P., Horton, J.K., and Wilson, S.H. (2000). The lyase activity of the DNA repair protein beta-polymerase protects from DNA-damage-induced cytotoxicity. *Nature* **405**, 807–810.

Sonoda, E., Okada, T., Zhao, G.Y., Tateishi, S., Araki, K., Yamaizumi, M., Yagi, T., Verkaik, N.S., van Gent, D.C., Takata, M., and Takeda, S. (2003). Multiple roles of Rev3, the catalytic subunit of polzeta in maintaining genome stability in vertebrates. *EMBO J.* **22**, 3188–3197.

Takanami, T., Nakamura, J., Kubota, Y., and Horiuchi, S. (2005). The Arg280His polymorphism in X-ray repair cross-complementing gene 1 impairs DNA repair ability. *Mutat. Res.* **582**, 135–145.

Ukai, A., Maruyama, T., Mochizuki, S., Ouchida, R., Masuda, K., Kawamura, K., Tagawa, M., Kinoshita, K., Sakamoto, A., Tokuhisa, T., and O-Wang, J. (2006). Role of DNA polymerase theta in tolerance of endogenous and exogenous DNA damage in mouse B cells. *Genes Cells* **11**, 111–121.

Yamazoe, M., Sonoda, E., Hochegger, H., and Takeda, S. (2004). Reverse genetic studies of the DNA damage response in the chicken B lymphocyte line DT40. *DNA Repair (Amst.)* **3**, 1175–1185.

Zan, H., Shima, N., Xu, Z., Al-Qahtani, A., Evinger Iii, A.J., Zhong, Y., Schimenti, J.C., and Casali, P. (2005). The translesion DNA polymerase theta plays a dominant role in immunoglobulin gene somatic hypermutation. *EMBO J.* **24**, 3757–3769.